The Astrophysical Journal, 703:L172–L177, 2009 October 1 doi:10.1088/0004-637X/703/2/L172

MMTF-Hα AND *HST*-FUV IMAGING OF THE FILAMENTARY COMPLEX IN ABELL 1795

Michael McDonald and Sylvain Veilleux[1]
Department of Astronomy, University of Maryland, College Park, MD 20742, USA
Received 2009 August 7; accepted 2009 September 3; published 2009 September 16

ABSTRACT

We have obtained deep, high spatial resolution images of the central region of Abell 1795 at Hα and [N II] λ6583 with the Maryland-Magellan Tunable Filter (MMTF), and in the far-ultraviolet (FUV) with the Advanced Camera for Surveys solar blind channel on the *Hubble Space Telescope* (*HST*). The superb image quality of the MMTF data has made it possible to resolve the known SE filament into a pair of thin, intertwined filaments extending for ∼50 kpc, with a width <1 kpc. The presence of these thin, tangled strands is suggestive of a cooling wake where runaway cooling is taking place, perhaps aided by an enhanced magnetic field in this region. The *HST* data further resolve these strands into chains of FUV-bright stellar clusters, indicating that these filaments are indeed sites of ongoing star formation, but at a rate ∼2 orders of magnitude smaller than the mass-deposition rates predicted from the X-ray data. The elevated [N II]/Hα ratio and large spatial variations of the FUV/Hα flux ratio across the filaments indicate that O-star photoionization is not solely responsible for the ionization. The data favor collisional heating by cosmic rays either produced in situ by magnetohydrodynamical processes or conducted from the surrounding intracluster medium.

Key words: cooling flows – galaxies: active – galaxies: clusters: individual (Abell 1795) – galaxies: elliptical and lenticular, cD – ISM: jets and outflows

1. INTRODUCTION

The absence of massive (∼100–1000 $M_\odot$ yr^{-1}) cooling flows in the cores of X-ray luminous galaxy clusters is often used as prime evidence that feedback plays an important role in regulating star formation and galaxy formation in dense environments (see, e.g., review by Veilleux et al. 2005). Energies of a few $\times 10^{49}$ erg per solar mass of stars formed are needed to explain the sharp cutoff at the bright end of the galaxy luminosity function. Starburst-driven winds are too feeble by a factor of several to fully account for the cutoff, so active galactic nucleus (AGN) feedback is invoked. The ubiquity of large "cavities" in the X-ray surface brightness of clusters with radio galaxies confirms that AGN outflows modify the thermodynamics of the intracluster medium (ICM; see review by Peterson & Fabian 2006). The relativistic gas injected into the ICM by the AGN has enough energy to quench the mass accretion of cooling flows, but the exact mechanism by which the energy in the radio bubbles turns into heat is still debated.

The presence of warm hydrogen in the form of line-emitting filaments extending from the brightest cluster galaxy (hereafter BCG) has been observed in many cooling flow clusters to date (e.g., Hu et al. 1985; Heckman et al. 1989; Crawford et al. 1999; Jaffe et al. 2005; Johnstone et al. 2005). However, while several intriguing ideas have been put forward, the origin of this gas and the mechanism for heating it are, as yet, unknown. Of all the galaxy clusters with known optical filaments, there is perhaps none quite so spectacular as Abell 1795. This cluster has been very extensively studied at a variety of wavelengths, leading to the discovery of a single, long (∼50 kpc) filament seen in Hα (Cowie et al. 1983; Maloney & Bland-Hawthorn 2001; Jaffe et al. 2005) and X-ray (Fabian et al. 2001; Crawford et al. 2005), a powerful, double-sided, radio jet (4C 26.42; van Breugel et al. 1984; Ge & Owen 1993) emanating from the central AGN, and a very disturbed, star-forming, central region (McNamara et al. 1996; Smith et al. 1997; Mittaz et al. 2001; Crawford et al. 2005).

As part of a survey of cooling flow clusters, we have carried out deep, high-resolution (delivered image quality, DIQ ∼ 0.″7) imaging of Abell 1795 at *Hα* and [N II] λ6583 using the Maryland-Magellan Tunable Filter (MMTF) on the Magellan-Baade 6.5 m telescope and in the far-ultraviolet (FUV) using the ACS solar blind channel (SBC) camera on the *Hubble Space Telescope* (*HST*). These data far surpass any previously available images of the filaments in this cluster in both depth and spatial resolution; this Letter describes the results from our analysis of these data. The results from the survey will be presented in future papers. The acquisition and reduction of the data on Abell 1795 are discussed in Section 2, followed by a description of the results (Section 3) and a discussion of the implications (Section 4). Throughout this Letter we assume a distance to Abell 1795 of 260 Mpc, based on a cosmology with $H_0 = 73$ km s^{-1} Mpc^{-1}, $\Omega_{\rm matter} = 0.27$, and $\Omega_{\rm vacuum} = 0.73$.

2. OBSERVATIONS AND DATA REDUCTION

2.1. Hα–Maryland-Magellan Tunable Filter

MMTF has a very narrow bandpass (∼5–12 Å) that can be tuned to any wavelength over ∼5000–9200 Å (Veilleux et al. 2009). Coupled with the exquisite image quality of Magellan, this instrument is ideal for detecting emission-line filaments in distant clusters. During 2008 April, we observed Abell 1795 for a total of 60 minutes each at $\lambda_{\rm H\alpha} = 6972.8$ Å, $\lambda_{\rm [N\,II]} = 6994.7$ Å, and $\lambda_{\rm continuum} = 7044$ Å. These data were reduced using the MMTF data reduction pipeline.[2] The continuum image was then PSF- and intensity-matched to the narrow-band images to allow for careful continuum subtraction.

[1] Also at Max-Planck-Institut für extraterrestrische Physik, Postfach 1312, D-85741 Garching, Germany.

[2] http://www.astro.umd.edu/∼veilleux/mmtf/datared.html

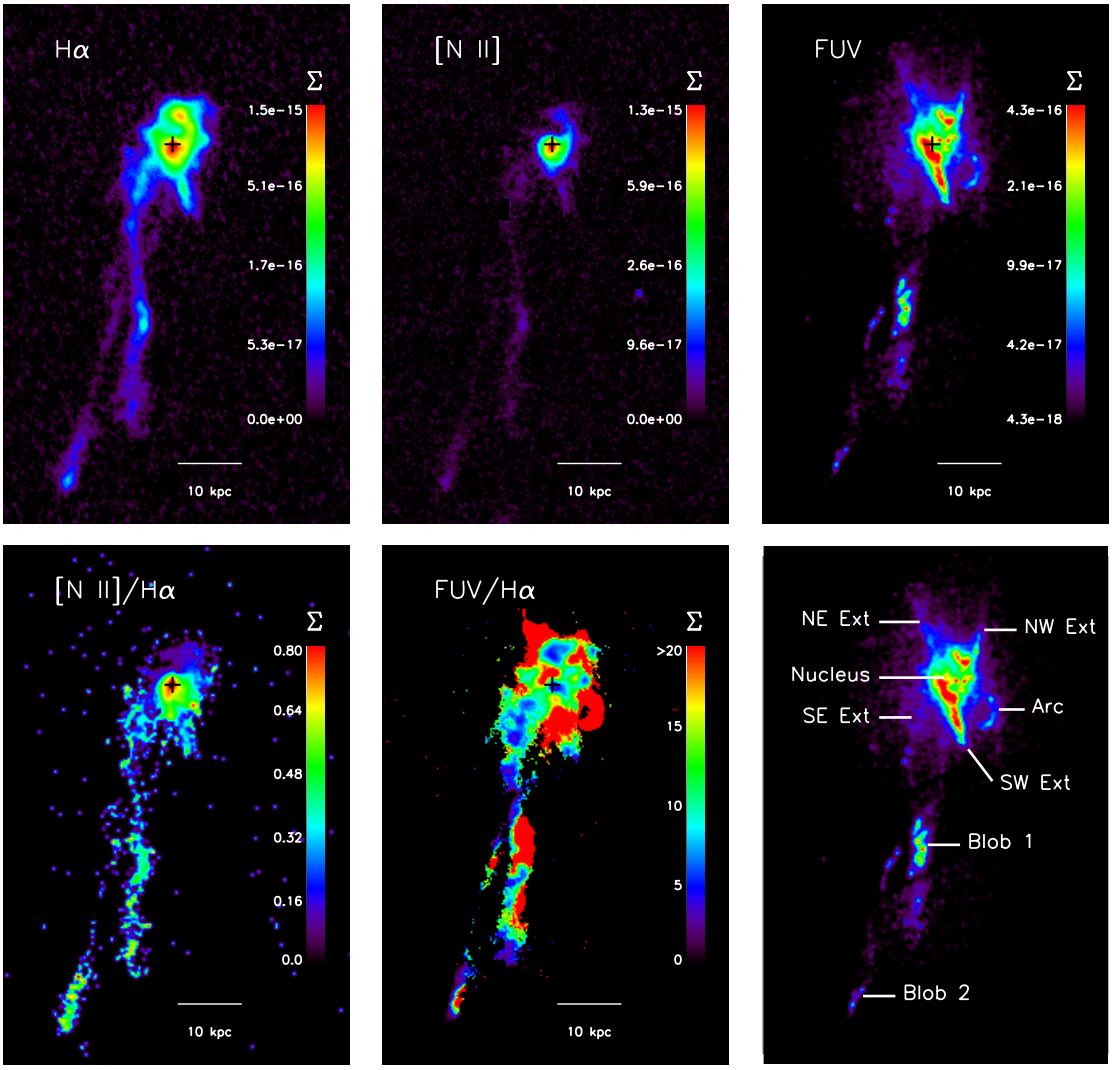

Figure 1. MMTF-Hα and [N II] λ6583 and *HST*/SBC FUV images of Abell 1795. The three upper panels show maps of the surface brightness, Σ, in units of erg s^{-1} cm^{-2} $arcsec^{-2}$. The lower left and center panels are [N II]/Hα and FUV/Hα ratio maps, respectively. In the latter image, the red shade represents regions where there is very little or no Hα coincident with the FUV emission. The bottom right panel outlines the terminology we use in this Letter, specifically in Table 1, for the different regions. The "central region" consists of all emission north of (and including) the SW extension. In all panels, the 10 kpc scale corresponds to 7.″9, and the black crosshair represents the centroid of optical emission, at $\alpha = 207.^{\circ}2188$, $\delta = 26.^{\circ}5929$.

2.2. *FUV*–Hubble Space Telescope *ACS/SBC*

FUV imaging was acquired using the ACS SBC on the *HST* in the F140LP bandpass, with a total exposure time of 1197 s. With the MMTF data already in hand, we were able to choose two different pointings of the 35″ × 35″ field of view to allow full coverage of the SE filament. Exposures with multiple filters are required to properly remove the known SBC red leak, which may be substantial in the central region due to the fact that the underlying galaxy is very luminous and red. However, we were unable to obtain complementary exposures in a redder SBC band for the filaments, due to scheduling constraints, and thus we proceed without removal of the offending light. The central UV fluxes have an associated error of ∼2.5% due to the underlying red galaxy (based on a preliminary analysis of additional FUV data of the central galaxy obtained by W. Sparks and collaborators).

3. RESULTS

Figures 1–3 show the newly acquired MMTF and *HST* data on Abell 1795. The most striking result is that the "SE filament," which has long been known (Cowie et al. 1983) is, in fact, a pair of thin, intertwined filaments in Hα. These filaments are ∼42″ and 35″ (52.9 and 44.1 kpc) in length, and their widths in Hα are unresolved (<0.″7 ∼ 1 kpc). The discovery of thin strands in the SE filament is reminiscent of magnetic field lines. A stronger than average magnetic field in the ICM could prevent the filament material from evaporating due to thermal conduction. The BCG in Abell 1795 is a bright double-jet radio-loud cD galaxy (4C 26.42) with therefore strong extended magnetic field (Ge & Owen 1993), but radio emission is not detected beyond ±6 kpc from the nucleus. We return to this issue in Section 4.

In the central region of Abell 1795, the Hα emission forms a ring, with a cavity slightly northeast of the BCG center (Figure 1). The morphology is very similar to that seen in the X-ray (Fabian et al. 2001). The cavity surrounds one of the radio jets emanating from the AGN, suggesting that it was created by recent AGN activity (Crawford et al. 2005). The very sharp extension directly to the southwest of the central region is coincident with the counter-jet. The jet appears to be efficiently heating the gas in this region (van Breugel et al. 1984). In

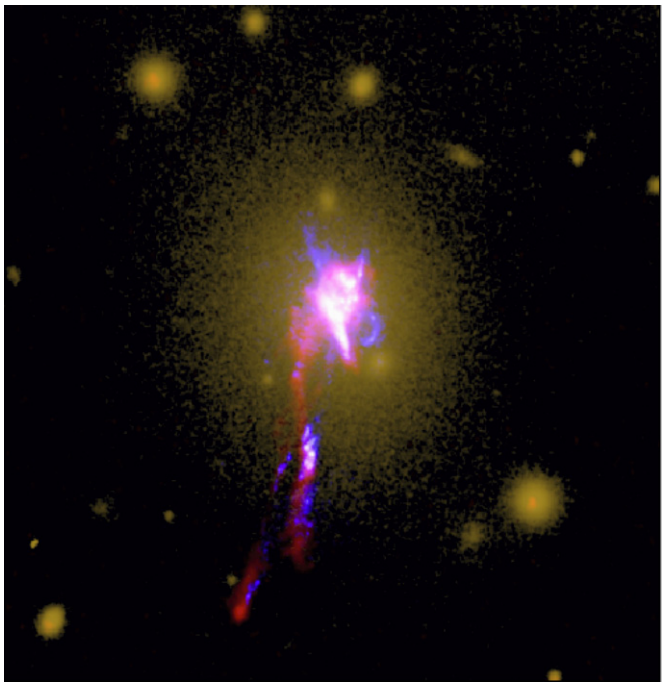

Figure 2. Color composite image of Abell 1795. The three colors represent the red continuum (yellow), Hα (red), and FUV (blue). The long SE filament is resolved into two intertwined filaments in Hα and FUV.

general, the Hα emission spatially correlates well with the X-ray emission in both the central regions and on larger scales to within the spatial resolution of the X-ray data.

The upper middle panel of Figure 1 reveals the distribution of [N II] in Abell 1795. All of the features that are seen in Hα are also visible in [N II], including both filaments, the short SW jet, the nucleus, and the cavity northeast of the nucleus. The ratio of [N II]/Hα, a measure of the relative importance of heating and ionization, is high and fairly uniform throughout the filaments ($\sim$0.35–0.55, see Table 1 and the lower left panel of Figure 1); this elevated ratio confirms earlier results (Crawford et al. 2005 and references therein) and seems inconsistent with photoionization by hot stars. [N II]/Hα is even higher in the nucleus, approaching unity, likely due to heating by the AGN, and drops northeast of the nucleus, where the jet has apparently cleared out a cavity. Given the MMTF bandwidth ($\sim$10 Å), we note that the [N II] image will also contain any Hα with relative velocity $>$785 km s^{-1}, and vice versa. However, since the typical velocity widths are $\sim$300 km s^{-1} in the filaments (e.g., Crawford et al. 2005), we do not expect interline contamination to be important.

In the FUV (Figure 1, upper right panel, and Figure 3), both strands are visible and, with the added resolution of *HST*, are resolved in some regions into chains of bright, compact sources—the sites of recent star formation (see also Crawford et al. 2005). The two brightest blobs seen in the filaments at Hα (blobs 1 and 2 in the nomenclature of Figure 1) break up into FUV point source and diffuse emission, but spatial offsets of $\sim$1–2 kpc are visible between the Hα and FUV emission centroids. This shift is particularly obvious in the FUV/Hα map in the lower middle panel of Figure 1. We do not believe this relative offset is due to errors in astrometry, since it was also noted in the earlier data of Crawford et al. (2005).

Most of the bright Hα features in the central region emit strong FUV, such as the nucleus, the ring, and the SW extension. However, there are features in the central region that are not

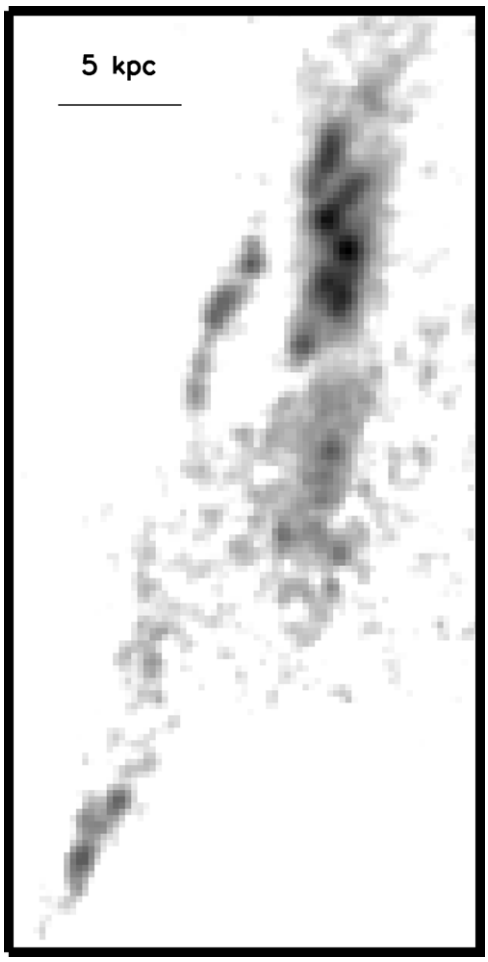

Figure 3. Close-up view of the crisscrossing filaments in the FUV showing both of the bright blobs. The brightest portions of the filaments break up into young UV-bright super star clusters.

common between the FUV and Hα data. In the FUV map, there are two northern extensions to the east and west (the NE and NW "extensions" in Figure 1), as well as a curved extension southwest of the central region (the "arc"). The emission in these regions is lumpy but largely unresolved into point sources. In Hα, there is a very bright and thick extension at the base of the SE filament which is not nearly as bright in the FUV. This region and other anomalous features are easily identified in the FUV/Hα map. (More details will be given in an upcoming paper where images of the central region of Abell 1795 in all three FUV bands of ACS/SBC are considered. This multiband analysis is beyond the scope of the present Letter.)

4. DISCUSSION

4.1. Origin and Power Source of Filaments

A number of very specific scenarios were put forward by Fabian et al. (2001) to explain the origin of the SE filament, taking into account that 4C 26.42 is in motion within the gravitational potential of the Abell 1795 cluster (Oegerle & Hill 2001; see also discussion in Crawford et al. (2005) and Rodríguez-Martínez et al. (2006)): (a) a cooling wake, produced by a cooling flow occurring around the moving cD galaxy (as in NGC 5044; David et al. 1994), (b) a "condensation trail" produced by the ram pressure of the radio source passing through the multiphase medium of the ICM and ISM of the host galaxy,

Table 1
Luminosities, Flux Ratios, and Inferred Star Formation Rates in the Central Region of Abell 1795

Region	$L_{H\alpha}$ (10^7 $L_\odot$)	$L_{[N\,II]}$ (10^7 $L_\odot$)	L_{UV} (10^7 $L_\odot$)	[N II]/Hα	UV/Hα	$SFR_{H\alpha}$ [a] ($M_\odot$ yr^{-1})	SFR_{UV} [a] ($M_\odot$ yr^{-1})
Total	5.49	1.97	8.07	0.36	14.7	<1.67	<2.66
SE filaments	0.72	0.26	1.47	0.36	20.3	0.22	0.48
Blob 1	0.25	0.09	0.70	0.38	28.4	0.08	0.23
Blob 2	0.16	0.09	0.16	0.53	10.0	0.05	0.05
Central region	4.77	1.72	6.61	0.36	13.8	<1.45	<2.18
Nucleus	0.12	0.10	0.06	0.81	4.4	<0.04	<0.02
NE extension	0.05	0.00	0.36	0.00	73.0	0.02	0.12
NW extension	0.05	0.00	0.16	0.00	33.3	0.02	0.05
SE extension	0.50	0.13	0.44	0.26	8.9	0.15	0.15
SW extension	1.00	0.48	1.85	0.48	18.5	0.30	0.61
Arc	0.03	0.00	0.28	0.00	102.8	0.01	0.09

Note. [a] Star formation rates derived using the prescriptions in Kennicutt (1998) assuming all of the Hα and UV emission, including that from the nucleus, is due to star formation; the value in the nucleus is therefore an upper limit.

(c) evaporation of cold gas ram pressure stripped from the cD galaxy, and (d) an accretion wake produced by the gravitational focusing effects of the moving cD galaxy on the ICM (e.g., Sakelliou et al. 1996).

Scenario (d) requires that the accreting ICM be gravitationally focused by the cD galaxy and cool into a wake. However, the relatively large sound speed of the hot gas makes it unlikely that this process alone can account for the presence of the long, thin, X-ray filament. In scenario (c), the material making up the filaments is interstellar medium (ISM) stripped from the cD galaxy. The large mass of hot gas in the filaments, $\sim 5 \times 10^9\ M_\odot$ (Fabian et al. 2001), and thin geometry of the filaments are hard to explain in this scenario. However, this does not exclude the possibility that *some* of the gas outside the cD galaxy is produced in this way (e.g., the broad base of the Hα filaments). Scenario (b) also presents some problems. As argued by Fabian et al. (2001), it seems unlikely that the cD galaxy plunging through the ICM would result in cooling, rather than heating, of the multiphase medium. Moreover we see no obvious connection in the data between the radio jets of 4C 6.42 and the long filaments.

By the process of elimination, these arguments seem to favor scenario (a). The very thin geometry of the Hα filaments points to highly nonlinear runaway cooling in this region. Potentially contributing heating/ionization sources in the filaments include (1) the central AGN, (2) hot young stellar population outside the cD galaxy, (3) X-rays from the ICM itself, (4) heat conduction from the ICM to the colder filaments, (5) shocks and turbulent mixing layers, and (6) collisional heating by cosmic rays. Arguments based on the AGN energetics and the line ratios in and out of the central region suggest that the AGN is not strongly influencing the ionization of the material much beyond the central region ($R \lesssim 6$ kpc). The long, thin geometry of the filaments and their quiescent velocity field (Crawford et al. 2005) seem to rule out ionization by shocks and/or turbulent mixing layers, while the relative weakness of high-ionization lines suggests that ionization by the X-ray ICM is also a small contributor. This leaves scenarios (2), (4), and (6) as the most plausible explanations for the dominant heating mechanism in the filaments.

The presence of FUV point sources in the filaments (Figure 3) lends support to scenario (2), but is there enough star formation to account for the observed Hα emission? To try to answer this question, we compare the FUV and Hα emission. Figure 4 shows the average Hα and FUV surface brightnesses of the brighter features defined in Figure 1. The Hα and FUV luminosities of these features are listed in Table 1. Assuming that the FUV and Hα star formation rate prescriptions of Kennicutt (1998) derived from the global properties of star-forming galaxies also apply individually to these features (we return to this assumption below), we find that the Hα and FUV surface brightnesses and luminosities of these features imply star formation rate surface densities and star formation rates which are generally consistent to within a factor of ∼2 of each other. The only exceptions are the arc and the NE and NW extensions, which are underluminous in Hα; this could be due to a lack of gas in these regions or other forms of continuum emission process. A detailed analysis of the central region using all three FUV bands of ACS/SBC (P.I.: W. Sparks) is in preparation. Under this assumption, the total Hα and UV-determined star formation rates are $\lesssim$1.7–2.7 $M_\odot$ yr^{-1}, with ∼0.2–0.5 $M_\odot$ yr^{-1} (∼15%–25%) contained in the filaments (Table 1). These numbers are lower than previous measurements of the total, integrated star formation rate of ∼5–20 $M_\odot$ yr^{-1} (Smith et al. 1997; Mittaz et al. 2001) and the estimate of $\lesssim$1 $M_\odot$ yr^{-1} of star formation in the filament (Crawford et al. 2005). These are all ∼2 orders of magnitude smaller than the predicted *Chandra*- and *XMM-Newton*-derived integrated mass deposition rates from the inner ICM (Ettori et al. 2002; Peterson et al. 2003).

The integrated Hα and FUV quantities discussed so far do not tell the full story: large spatial variations of the FUV/Hα ratio are seen on smaller scale (see the lower middle panel of Figure 1 and pixel-to-pixel surface brightness measurements of Figure 4). These spatial variations may be due to a number of effects, including differential dust extinction, variations in star formation history (SFH; age of burst, decay timescale) or initial mass function (IMF), complex geometry of the gas relative to the ionizing stars, and contributions from non-stellar processes to the FUV and Hα emission. Extinction corrections would boost the FUV fluxes relative to Hα and therefore could account for regions with anomalously small FUV/Hα ratios. Published data on the filaments suggest relatively modest extinctions, however (e.g., Crawford et al. 2005). Variations in the SFH or IMF change the relative importance of ionizing and non-ionizing stars and may account for variations in both directions of the FUV/Hα flux ratio. Our data do not provide strong constraints on these parameters. Geometrical effects are undoubtedly important in

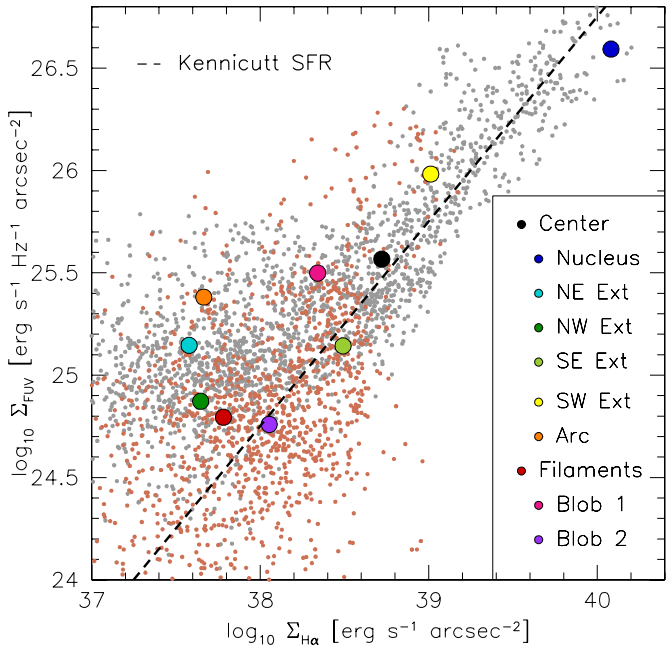

Figure 4. FUV surface brightness, $\Sigma_{\rm FUV}$, vs. Hα surface brightness, $\Sigma_{\rm H\alpha}$, in Abell 1795. The dashed line represents the expected relation between the global $\Sigma_{\rm H\alpha}$ and $\Sigma_{\rm FUV}$ for star-forming galaxies (Kennicutt 1998). The larger symbols show the average surface brightness over the brighter features defined in Figure 1. The background distribution of points shows the 2×2 pixel-by-pixel surface brightness measurements for the central region (gray) and filaments (light red).

some regions, particularly in blobs 1 and 2, where spatial offsets of ∼1–2 kpc are visible between the Hα and FUV emission centroids. In these blobs, the Kennicutt (1998) prescriptions may severely underestimate the number of FUV-bright stars needed to account for the Hα emission; processes other than photoionization by hot stars appear needed to account for the observed Hα at these locations (the recombination timescale is at least an order of magnitude shorter than the dynamical timescale to move ∼1–2 kpc, unless the density of the Hα filaments is much less than ~ 1 cm^{-3}).

As mentioned in Section 3, additional heating sources also appear needed to explain the unusually strong low-ionization lines detected in the blobs and in between them (e.g., Hu et al. 1985; Crawford et al. 2005; Figure 1). Two heating processes remain viable: (4) heat conduction from the ICM to the colder filaments and (6) collisional heating by cosmic rays. The relative importance of these processes critically depends on the strength of the magnetic field in the filaments. Strong magnetic fields could shield the cooling ICM gas from re-heating by conduction with the hot ICM (scenario (4)), creating long tubes of cool, dense gas. Runaway star formation would take place along these magnetic field lines, where the gas is cooling and condensing to high enough density to become Jeans unstable. The long, thin geometry of the Hα SE filaments and detection of embedded FUV-bright stellar clusters in these filaments are consistent with this picture.

Ferland et al. (2008, 2009) have recently examined the question of the importance of heating by energetic particles or dissipative magnetohydrodynamic (MHD) waves in the central nebulae of massive clusters. The energetic particles contributing to the heating of the filaments in this scenario may either be produced in situ by MHD processes or conducted in from the surrounding ICM. Given our previous discussion, we speculate that the optical emission in the SE filaments of Abell 1795 may naturally be explained by these heating processes. The magnetic field in the filaments may represent residual magnetic field originally associated with the radio galaxy but now entrained in the ICM flow. If this is the case, the crisscrossing geometry of the SE filaments may reflect precession of the radio jets or the orbital motion of the cD galaxy in the cluster potential.

Finally, we end with a cautionary note: our data do not provide quantitative constraints on the strength of the purported ICM magnetic field. The possibility of runaway star formation unaided by magnetic field cannot be ruled out. In fact, the filaments seen in Abell 1795 shares a morphological resemblance with the narrow cold streams seen feeding galaxies in recent high-resolution numerical simulations of the early universe (e.g., Ceverino et al. 2009).

5. CONCLUDING REMARKS

Using deep, high-resolution Hα, [N II] λ6584, and FUV data, we have discovered that the SE filament in Abell 1795 is in fact two intertwined filaments of ionized hydrogen. The most plausible origin for these filaments is a wake of cooling ICM behind the moving cD galaxy in Abell 1795. The narrowness of the strands suggest highly nonlinear runaway cooling of the ICM. Their tangled morphology suggests that the infalling gas may be interacting with enhanced magnetic fields, allowing for less efficient energy conduction and faster cooling in this region. We observe knots of UV-bright point sources along these filaments, indicating star formation at a rate of $\sim 0.5\,M_{\odot}$ yr^{-1} in the filaments. The large spatial variations of the FUV/Hα ratio and enhanced low ionization lines suggest that O-star photoionization is not the sole source of heating of this gas; collisional heating by energetic particles is another likely contributor. A deeper understanding of the origin of the filaments of Abell 1795 will require detailed MHD modeling and observations to constrain the purported magnetic field, both of which are beyond the scope of the present Letter. It is also not clear yet whether this scenario applies to cooling flow clusters in general. We plan to address this issue in upcoming papers using a representative set of massive clusters.

Support for this work was provided to M.M. and S.V. by NSF through contract AST 0606932 and by NASA through contract HST GO-1198001A. S.V. also acknowledges support from a Senior Award from the Alexander von Humboldt Foundation and thanks the host institution, MPE Garching, where this Letter was written. We thank D. S. N. Rupke, C. S. Reynolds, E. Ostriker, H. Netzer, and M. C. Miller for useful discussions, and are particularly grateful to W. Sparks for letting us examine F150LP and F165LP images of the central region of Abell 1795 obtained under *HST*/PID 11681.

REFERENCES

Ceverino, D., Dekel, A., & Bournaud, F. 2009, MNRAS, submitted (arXiv:0907.3271)
Cowie, L. L., Hu, E. M., Jenkins, E. B., & York, D. G. 1983, ApJ, 272, 29
Crawford, C. S., Allen, S. W., Ebeling, H., Edge, A. C., & Fabian, A. C. 1999, MNRAS, 306, 85
Crawford, C. S., Sanders, J. S., & Fabian, A. C. 2005, MNRAS, 361, 17
David, L. P., Jones, C., Forman, W., & Daines, S. 1994, ApJ, 428, 544
Ettori, S., Fabian, A. C., Allen, S. W., & Johnstone, R. M. 2002, MNRAS, 331, 635
Fabian, A. C., Sanders, J. S., Ettori, S., Taylor, G. B., Allen, S. W., Crawford, C. S., Iwasawa, K., & Johnstone, R. M. 2001, MNRAS, 321, L33
Ferland, G. J., et al. 2008, MNRAS, 386, L72

Ferland, G. J., et al. 2009, MNRAS, 392, 1475
Ge, J. P., & Owen, F. N. 1993, AJ, 105, 778
Heckman, T. M., Baum, S. A., van Breugel, W. J. M., & McCarthy, P. 1989, ApJ, 338, 48
Hu, E. M., Cowie, L. L., & Wang, Z. 1985, ApJS, 59, 447
Jaffe, W., Bremer, M. N., & Baker, K. 2005, MNRAS, 360, 748
Johnstone, R. M., et al. 2005, MNRAS, 382, 1246
Kennicutt, R. C., Jr. 1998, ARA&A, 36, 189
Maloney, P. R., & Bland-Hawthorn, J. 2001, ApJ, 553, L129
McNamara, B. R., Wise, M., Sarazin, C. L., Jannuzi, B. T., & Elston, R. 1996, ApJ, 466, L9
Mittaz, J. P. D., et al. 2001, A&A, 365, L93
Oegerle, W. R., & Hill, J. M. 2001, AJ, 122, 2858
Peterson, J. R., & Fabian, A. C. 2006, Phys. Rep., 427, 1
Peterson, J. R., Kahn, S. M., Paerels, F. B. S., Kaastra, J. S., Tamura, T., Bleeker, J. A. M., Ferrigno, C., & Jernigan, J. G. 2003, ApJ, 590, 207
Rodríguez-Martínez, M., Velázquez, P. F., Binette, L., & Raga, A. C. 2006, A&A, 448, 15
Sakelliou, I., Merrifield, M. R., & McHardy, I. M. 1996, MNRAS, 283, 673
Smith, E. P., Bohlin, R. C., Bothun, G. D., O'Connell, R. W., Roberts, M. S., Neff, S. G., Smith, A. M., & Stecher, T. P. 1997, ApJ, 478, 516
van Breugel, W., Heckman, T., & Miley, G. 1984, ApJ, 276, 79
Veilleux, S., Cecil, G., & Bland-Hawthorn, J. 2005, ARA&A, 43, 769
Veilleux, S., et al. 2009, AJ, submitted (arXiv:0908.1629)